HHS Public Access

Author manuscript

J Neurosci Res. Author manuscript; available in PMC 2015 June 29.

Published in final edited form as:

J Neurosci Res. 2012 December ; 90(12): 2306–2316. doi:10.1002/jnr.23112.

Characterization of Cellular Protective Effects of ATP13A2/PARK9 Expression and Alterations Resulting From Pathogenic Mutants

Jason P. Covy[1], **Elisa A. Waxman**[2], and **Benoit I. Giasson**[3,★]

[1]Department of Cellular and Molecular Physiology, Stanford University, Stanford, California

[2]Research and Development Department, Medical Diagnostic Laboratories LLC, Hamilton, New Jersey

[3]Department of Neuroscience, University of Florida, Gainesville, Florida

Abstract

Mutations in ATP13A2, which encodes a lysosomal P-type ATPase of unknown function, cause an autosomal recessive parkinsonian syndrome. With mammalian cells, we show that ATP13A2 expression protects against manganese and nickel toxicity, in addition to proteasomal, mitochondrial, and oxidative stress. Consistent with a recessive mode of inheritance of gene defects, disease-causing mutations F182L and G504R are prone to misfolding and do not protect against manganese and nickel toxicity because they are unstable as a result of degradation via the endoplasmic reticulum-associated degradation (ERAD)-proteasome system. The protective effects of ATP13A2 expression are not due to inhibition of apoptotic pathways or a reduction in typical stress pathways, insofar as these pathways are still activated in challenged ATP13A2-expressing cells; however, these cells display a dramatic reduction in the accumulation of oxidized and damaged proteins. These data indicate that, contrary to a previous suggestion, ATP13A2 is unlikely to convey cellular resilience simply by acting as a lysosomal manganese transporter. Consistent with the recent identification of an ATP13A2 recessive mutation in Tibetan terriers that develop neurodegeneration with neuronal ceroid lipofucinoses, our data suggest that ATP13A2 may function to import a cofactor required for the function of a lysosome enzyme(s).

Keywords

ATP13A2; Kufor-Rakeb; Parkinson’s disease; PARK9; oxidative stress

Parkinson’s disease (PD) is the most common movement disorder, affecting over 6 million people worldwide. PD typically afflicts individuals over the age of 55 years; however, small but significant numbers of cases present with a juvenile or early onset (Gelb et al., 1999; Simuni and Hurtig, 2000). The clinical features of PD include bradykinesia, postural instability, resting tremor, and rigidity, which are associated predominantly with the

★Correspondence to: Dr. Benoit I. Giasson, Department of Neuroscience, Center for Translational Research in Neurodegenerative Diseases, University of Florida, 1275 Center Drive, BMS Building J-497, P.O. box 100159, Gainesville, FL 32610-0244. bgiasson@ufl.edu.

progressive loss of dopaminergic neurons in the substantia nigra pars compacta (Cromford et al., 1995; Forno, 1996; Forman et al., 2005). Although most PD cases are idiopathic, growing numbers of gene loci, referred to as *PARK1–18*, have been associated with familial and sporadic forms of the disease (Lesage and Brice, 2009; Westerlund et al., 2010; Martin et al., 2011). In addition to genetic defects, a range of environmental and occupational features, such as pesticides, to more ubiquitous metals, such as manganese, have been implicated as risk factors in PD (Lai et al., 2002; Dick et al., 2007; Elbaz et al., 2009).

Mutations in ATP13A2/PARK9 were identified as the cause of Kufor-Rakeb syndrome, a juvenile recessive multisystemic neurodegenerative disorder with prominent parkinsonism (Hampshire et al., 2001; Williams et al., 2005; Ramirez et al., 2006). Splicing, short duplication, or deletion mutations resulting in truncated forms of the protein were found in the original family, along with several other families and sporadic cases (Ramirez et al., 2006; Paisan-Ruiz et al., 2010; Crosiers et al., 2011; Eiberg et al., 2011). Several recessive missense mutations (F182L, L1059R, and G877R) in ATP13A2 have been found in patients with Kufor-Rakeb syndrome (Ning et al., 2008; Park et al., 2011; Santoro et al., 2011), and an additional recessive mutation (G504R) was identified in an individual with juvenile PD (Di et al., 2007).

ATP13A2 is a ubiquitously expressed 1,180-aminoacid protein with a putative 10-transmembrane topology (see Fig. 1) belonging to the P-type superfamily of ATPase transporters, named according to the phosphorylation of an intermediate on a D residue during the enzymatic cycle (Axelsen and Palmgren, 1998; Kuhlbrandt, 2004; Schultheis et al., 2004; Ramirez et al., 2006; Weingarten et al., 2012). These enzymes use ATP hydrolysis typically to generate gradients of inorganic cations across membranes, although some of these ATPase also transport aminophospholipids (Axelsen and Palmgren, 1998; Kuhlbrandt, 2004). ATP13A2 belongs to the P5 subfamily of P-type ATPases, which is the least well-characterized subfamily. P5 ATPases appear to be expressed only in eukaryotes, and, to date, no known substrates have been directly identified (Axelsen and Palmgren, 1998; Kuhlbrandt, 2004; Schultheis et al., 2004). ATP13A2 appears to be localized predominantly to lysosomes (Ramirez et al., 2006; Park et al., 2011; Tan et al., 2011; Ugolino et al., 2011; Ramonet et al., 2012), and, for yeast, a homologue termed *YPK9* has been shown to be protective against the toxicity of certain heavy metals, including manganese, cadmium, nickel, and selenium (Gitler et al., 2009; Schmidt et al., 2009). In some mammalian cells, ATP13A2 expression has also been shown to suppress manganese toxicity associated with a relative reduction in the levels of intracellular manganese (Tan et al., 2011).

Here we show that the disease causing mutations F182L and G504R in ATP13A2 leads to their aberrant proteasomal degradation, likely because of protein misfolding and aggregation. These findings are consistent with the recessive mode of inheritance of gene defects. Furthermore, we assessed the effects of ATP13A2 on the toxicity of heavy metals and other cellular stresses in mammalian cells. We confirm with mammalian cells that ATP13A2 confers protection against the heavy metals manganese and nickel, but it also has a protective role against many other cellular stresses, indicating a much broader protection against neurotoxicity than was previously thought.

MATERIALS AND METHODS

Antibodies and Reagents

Anti-ATP13A2 antibody A9732 was produced in rabbit against a synthetic peptide corresponding to amino acids 1162–1180 of human ATP13A2 conjugated to keyhole limpet hemocyanin (KLH; Sigma, St. Louis, MO). Anti-V5 antibody was purchased from Invitrogen (Carlsbad, CA). Antiphospho-SAPK/JNK (Thr183/Tyr185; clone 81E11), anti-SAPK/JNK, antiphospho-ERK1/2 (Thr202/Tyr204; clone D13.14.4E), anti-ERK1/2 (clone 137F50), cleaved PARP (Asp 214), antipoly(ADP-ribose) polymerase (PARP; clone 46D11), anticleaved caspase-3 (Asp 175; clone 5A1E), anticaspase 3, and anticalnexin antibody (clone C5C9) rabbit antibodies were purchased from Cell Signaling Technology (Danvers, MA). Apotrack cytochrome c apoptosis WB antibody cocktail was purchased from Abcam (Cambridge, MA). Anti-Lamp1 mouse monoclonal antibody was obtained from BD Biosciences (San Jose, CA). Antiactin (clone C4) is a purified mouse monoclonal antibody (Millipore, Billerica, MA) that reacts with all six isoforms of vertebrate actin. 1-Methyl-4-phenylpyridinium (MPP^+) dihydrochloride, rotenone, and cycloheximide were obtained from Sigma. MG132 was purchased from EMD Biosciences (Gibbstown, NJ).

Cloning of Human ATP13A2 Constructs

The full-length human wild-type (WT) ATP13A2 cDNA without a terminal stop codon was amplified by PCR using Taq polymerase AccuPrimeSuperMix (Invitrogen) with the following oligonucleotides: GCCGGCATGAGCGCAGACAGCAGCCCTCTC and CCTCAGGGGCCGGCGGGCAGCGGCGGCC. The DNA product was cloned by topo-isomerase reaction into the shuttling vector pCR8/GW/TOPO. Plasmids with ATP13A2 mutation corresponding to the F182L, G504R, or D513N amino acid substitution were generated by using the QuickChange Site Directed Mutagenesis Kit (Stratagene, La Jolla, CA). The plasmid sequences were verified by DNA sequencing as a service offered by the DNA Sequencing Facility of the University of Pennsylvania. WT and mutant full-length ATP13A2 cDNAs were introduced into the pEF-DEST51 vector by recombinase reaction using LR Clonase II enzyme (Invitrogen) to generate a plasmid expressing C-terminal V5-tagged protein.

Cell Culture

Human embryonic kidney 293T cells (293T) and human neuroblastoma cells (NLF) were cultured in Dulbecco’s modified medium (DMEM) high glucose (4.5 g/liter) supplemented with 10% fetal bovine serum (FBS), 100 U/ml penicillin, 100U/ml streptomycin, and 2 mM L-glutamine.

Generation of Stable NLF Cells Lines Expressing WT ATP13A2 and Cell Viability Studies

Human full-length WT ATP13A2/pEF-DEST51 construct was used to transfect NLF cells using Lipofectamine 2000 reagent (Invitrogen), following the manufacturer’s protocol. Stably expressing clones were isolated and selected with Blasticidin S (Invitrogen) at 10 μg/ml and screened by Western blotting analysis for the expression of ATP13A2 using anti-V5 antibody.

To assess cell viability of stable cell lines, native NLF cells or NLF cell lines expressing WT ATP13A2 were cultured separately into six-well plates. Each cell type was treated for 24 hr in sextuplicate with DMEM/FBS containing the indicated challenges. After treatment, the medium from each well was collected into separate 1.5-ml microfuge tubes. The cells remaining in the wells were trypsinized and harvested in corresponding microfuge tubes. Cells were pelleted and resuspended in fresh DMEM/FBS, and then a threefold volume of Trypan blue solution (Sigma) was added. Cells were counted manually with a hemacytometer and an Olympus CKX41 microscope. For statistical analysis of each treatment in comparison with NLF control cells, one-way ANOVA followed by a Tukey-Kramer post hoc analysis was performed.

To assess relative cellular injury in NLF cells that were transiently transfected with constructs expressing WT, F182L, G504R, or D513N ATP13A2, cells were cotransfected with a 3:1 ratio of ATP13A2 vector to pEGFPF-CI plasmid (Clontech, Palo Alto, CA) using Lipofectamine 2000 transfection reagent (Invitrogen), following the manufacturer's protocol. After challenge, cells were fixed with 4% paraformadehyde/PBS, stained with 4′, 6-diamidino-2-phenylindole (DAPI; 2 μg/ml), and coverslips were mounted with Fluoromount-G (Southern Biotechnology, Birmingham, AL). Images were captured with an Olympus BX51 fluorescence microscope mounted with a DP71 digital camera (Olympus, Center Valley, PA). The percentage of green fluorescent protein (GFP)-positive cells that displayed condensed nuclear chromatin was determined by analyzing more than three fields with more than 100 cells per field. For statistical analysis of each treatment in comparison with NLF transected with only pEGFPF-CI plasmid, one-way ANOVA followed by a Tukey-Kramer post hoc analysis was performed.

Western Blotting Analysis

Proteins were resolved on sodium dodecyl sulfate (SDS)-polyacrylamide gels by SDS-PAGE and electrophoretically transferred onto nitrocellulose membranes (Bio-Rad, Hercules, CA) in buffer containing 190 mM glycine, 25 mM Tris base, and 10% methanol. Membranes were blocked in Tris-buffered saline (TBS) with 5% dry milk and incubated overnight with primary antibodies diluted in TBS/5% bovine serum albumin (BSA). Each incubation was followed by goat anti-mouse-conjugated horseradish peroxidase (HRP; Amersham Biosciences, Piscataway, NJ) or goat anti-rabbit-conjugated HRP (Cell Signaling Technology), and immunoreactivity was detected by using chemiluminescent reagent (NEN, Boston, MA) followed by exposure onto X-ray film.

Steady-State Protein Analysis and Relative Stability

293T and NLF cells were cultured in 35-mm dishes and transfected with WT, F182L, or G504R ATP13A2/pDEST51 constructs using Lipofectamine 2000 transfection reagent, following the manufacturer's protocol. For steady-state protein analysis, at 30 hr posttransfection, cells were rinsed with PBS and harvested in 3% SDS/50 mM Tris, pH 7.5. For assessment of relative stability, 30 hr posttransfection, cells were treated with 100 μM cycloheximide and harvested at indicated time points. Total cell lysates were heated at 100°C for 10 min, quantified by using the bicinchoninic acid (BCA) protein assay (Thermo Scientific, Rockford, IL), and analyzed by Western blotting with the anti-V5 and antiactin

monoclonal antibodies. Quantification was performed by standardizing densitometry of ATP13A2 anti-V5 immunoreactivity relative to actin and as a percentage of ATP13A2 at time zero.

Double-Immunofluorescence Analysis

Cells were fixed with 4% paraformaldehyde for 15 min, followed by 100% MeOH at −20°C for 30 min. After washes with PBS, coverslips were blocked with PBS containing 3% BSA, 1% dry milk, and 1% fish gelatin for 1 hr, followed by primary antibodies diluted in blocking solution for 2 hr at room temperature. After PBS washes, coverslips were incubated in secondary antibodies conjugated to Alexa 488 or Alexa 594 for 1 hr. Nuclei were counterstained with Hoechst trihydrochloridetrihydrate 33342 (Invitrogen), and coverslips were mounted using Fluoromount-G. Confocal microscopic images were captured on a Zeiss Axiovert 200M inverted confocal microscope mounted with a Zeiss LSM510 Meta NLO digital camera utilizing Zeiss LSM510 Meta V3.2 confocal microscope software (Zeiss, Thornwood, NY). Confocal images were captured with ×63 oil optics. Representative images were of one Z-plane of <0.7 μm.

Cellular Fraction of Cytochome C

Fractionation was carried out using the Mitoscience (Cambridge, MA) Cell Fractionation Kit according to the manufacture's protocol. Briefly, cells were plated in 10-cm^2 dishes, and, when semiconfluent (~2.5×10^6 cells/plate), the medium was saved and combined with cells after detachment with trypsin. After centrifugation, cells counts were normalized across conditions at 6.6×10^6 cells/ml, and centrifugation and sequential extraction of cellular, mitochondrial, and nuclear fractions were carried out. Identification of each fraction as well as cytochrome c was accomplished by Western blotting analysis utilizing the Apotrack cytochrome c apoptosis WB antibody cocktail.

Measurement of Glutathione Incorporation

Glutathione incorporation was assessed by incorporation of biotinylated glutathione ethyl ester (BioGEE; Invitrogen) according to the manufacturer's protocol. Briefly, BioGEE (250 μM) was added to the medium and incubated for 1 hr, followed by challenge with the indicated cellular stress. Cells were scraped and spun down in their own media to allow for collection of detached cells, washed twice in PBS, and lysed in CSK buffer (100 mM NaCl, 50 mM Tris, pH 7.5, 2 mM EDTA, 1% Triton X-100) with protease inhibitors. Lysates were spun at 4°C for 10 min, and a 1:1 addition of 6% SDS was added to the soluble fraction. Protein concentrations were determined by BCA assay, and samples were analyzed by Western blotting analysis using streptavidin-HRP (Cell Signaling Technology).

RESULTS

Generation of Stable Cells Lines That Express ATP13A2

To study the effects of ATP13A2 in mammalian cells, we generated stable cell lines of NLF human neuroblastoma that overexpress human ATP13A2 as described in Materials and Methods. Three clones (clones NLF-P9 No. 1, NLF-P9 No. 3, and NLF-P9 No. 14) that express similar levels of WT ATP13A2 were selected for these studies (Fig. 2). These

clones were shown to express ATP13A2 by immunoblotting analysis using both a V5-tag antibody and an antibody specific for ATP13A2 (Fig. 2). Despite repeated attempts, we were not able to establish stable clones expressing F182L or G504R mutant of ATP13A2 (for details see below).

ATP13A2 Protects Against Manganese and Nickel Toxicity in Mammalian Cells

To assess whether overexpression of ATP13A2 confers protection against manganese and nickel toxicity in mammalian cells, we challenged native NLF cells and the stable clones expressing ATP13A2 with increasing concentration of these divalent metals. All stable clones showed substantial protection against manganese and nickel challenge (Fig. 3A,B). Because we were not able to generate stable cell lines expressing F182L or G504R ATP13A2 (see below), we performed toxicity analysis for manganese and nickel using transiently transfected cells and assayed for the appearance of condensed nuclei as a measure of cellular health. For comparison, we also included an enzymatic “dead” version of ATP13A2 in which the D513 residue that is phosphorylated during the catalytic cycle within the conserved DKTGT motif (Kuhlbrandt, 2004) is mutated to an N (D513N mutant). The expression of WT ATP13A2, but not that of F182L, G504R, or D513N ATP13A2, resulted in protection against manganese and nickel toxicity (Fig. 4).

Pathogenic ATP13A2 Mutants F182L and G504R Demonstrate Reduced Protein Stabilities, Protein Aggregation, and Protein Degradation by the Proteasome

Despite multiple attempts, we were unable to establish stable cells lines expressing F182L or G504R ATP13A2. To confirm that these mutants could be expressed and to determine their relative expression level compared with WT ATP13A2, cells were transiently transfected in parallel with WT, F182L, or G504R ATP13A2. Both F182L and G504R ATP13A2 could be expressed, but their levels were substantially lower in both NLF and 293T cells (Fig. 5A). To assess whether this lower expression was caused by enhanced degradation, we performed ^{35}S-methionine labeling pulse-chase experiments, but, despite numerous attempts, we were unable to immunoprecipitate ATP13A2 reproducibly and quantitatively, likely because of the complex topology of this transmembrane protein. As an alternative method to compare the degradation of WT and mutant ATP13A2, we wanted to utilize protease inhibitors. To this end, an analysis of the typical turnover of WT ATP13A2 was first required to establish the period of protease inhibition needed for this analysis. The relative turnover of WT ATP13A2 was assessed by using cycloheximide to inhibit translation, which showed that the relative half-life of WT ATP13A2 was approximately 6 hr (Fig. 5B,C). Therefore, if the lower levels of expression of F182L and G504R ATP13A2 were due to increased degradation, 6 hr of protease inhibitor treatment should be sufficient to observe the stabilization of these proteins. 293T cells transfected with WT, F182L, or G504R ATP13A2 were treated for 6 hr with the proteasome inhibitor MG132 and the lysosome inhibitor NH_4Cl. MG132, but not NH_4Cl, treatment significantly increased the levels of F182L and G504R ATP13A2, which appeared mostly as a higher molecular weight smear, suggesting protein misfolding and aggregation. To investigate further the nature of the effects of these pathogenic mutants, we performed confocal double-immunofluorescence microscopic analysis with specific organelle markers. Analysis with Lamp1 antibodies showed that WT ATP13A2 was localized predominantly to lysosomes (Fig. 6), as

previously reported (Ramirez et al., 2006; Park et al., 2011; Tan et al., 2011; Ugolino et al., 2011; Ramonet et al., 2012). In contrast both the F182L and the G504R mutants were localized predominantly to the endoplasmic reticulum as observed from calnexin localization (Fig. 6). Treatment with MG132 for 6 hr did not alter the localization of WT or mutant ATP13A2; however, there was an increase in the intensity of F182L and G504R ATP13A2, which in some cases appear to form aggregates (data not shown).

ATP13A2 Protection Against Other Cellular Stresses

To assess whether the protection conferred by ATP13A2 was specific to heavy metals, stable cell lines expressing ATP13A2 were exposed to stresses that have been linked to pathways associated with PD. Because oxidative stress has long been implicated in the etiology of PD (Zhang et al., 2000; Giasson et al., 2002), we tested whether ATP13A2 could protect against this type of insult by challenging cells with H_2O_2. ATP13A2 expression significantly protected against this type of oxidative damage (Fig. 7A). Mitochondrial complex I dysfunction is associated with PD (Dawson and Dawson, 2003; Ramsey and Giasson, 2007; Henchcliffe and Beal, 2008), so we assessed the effects of expressing ATP13A2 on the toxicity of the complex I inhibitors rotenone and MPP^+ dihydrochloride. ATP13A2 demonstrated protection against both of these challenges (Fig. 7B,C), but the window of protection was much smaller against MPP^+; it was significant only at 20 μM. Proteasomal dysfunction has also been associated with PD (Dawson and Dawson, 2003; Giasson and Lee, 2003), and ATP13A2 also demonstrated significant protection against the toxicity of the proteasome inhibitor MG132 (Fig. 7D).

Expression of ATP13A2 Does Not Prevent Intracellular Stress or Caspase Activation but Reduces Oxidative Damage

To begin to investigate the mechanism by which ATP13A2 protects against adverse cellular stress, signal transduction pathways that are typically induced by these conditions were analyzed (Fig. 8A). For these comparative studies, we studied a cell line (NLF P9–14) that overexpresses ATP13A2 vs. native NLF cells under challenges with either H_2O_2 or $MnCl_2$. Both cell lines expressed equal levels of ERK and JNK, but, under basal conditions, phospho-ERK levels were lower in NLF P9–14 cells. After manganese treatment, the levels of phospho-JNK increased in both NLF and NLF P9–14 cells, indicating that expression of ATP13A2 does not prevent the cell from being stressed or sensing these stresses. Both cell lines expressed equivalent levels of pro-caspase-3, but, under challenged conditions, NLF P9–14 cells generated higher levels of cleaved active caspase-3 compared with native NFL cells even under basal conditions. Consistent with this finding, under challenged conditions, NLF P9–14 cells also produced higher levels of the downstream substrate of caspase-3, cleaved PARP. To assess the pathway upstream of caspase-3, we assayed the release of cytochrome C from the mitochondria (Fig. 8B). The cells overexpressing ATP13A2 (NLF P9–14) demonstrated a greater release of cytochrome C under stressed conditions, especially for $MnCl_2$ treatment.

To understand better the mechanism of ATP13A2-associated protection, we used the biotinylated glutathione ethyl ester (BioGEE) assay to assess intracellular oxidative stress. Under conditions of oxidative stress, cells can transiently incorporate glutathione into

proteins, and this cell-permeable biotinylated analog can be used to detect this modification. Treatment with either H_2O_2 or $MnCl_2$ significantly increased the level of glutathione incorporation in several proteins in native NLF cells, and this was greatly reduced in cells overexpressing ATP13A2 (NLF P9–14; Fig. 8C).

DISCUSSION

PD is an insidious neurodegenerative disorder that is characterized by the selective demise of specific neuronal populations, including dopaminergic neurons of the substantia nigra, and is associated with an impairment of motor functions. However, PD is also associated with a range of nonmotor symptoms (Chaudhuri et al., 2006; Poewe, 2008), and there is increasing awareness that the loss of neurons in PD is not exclusive to nigral dopaminergic neurons, insofar as several other neuronal populations are also affected (Cromford et al., 1995; Forno, 1996; Forman et al., 2005; Braak et al., 2006). Most cases of PD are sporadic, but many disease-causing genes have been identified, and these discoveries have led to important breakthroughs in understanding the etiology of PD (Forman et al., 2005; Lesage and Brice, 2009; Westerlund et al., 2010).

Most disease-causing mutations reported for ATP13A2/PARK9, including splicing, short duplication, deletion, or insertion mutations result in truncated forms of the protein that clearly disrupt protein function, and most of these erroneous products have been shown to be retained in the endoplasmic reticulum and degraded by the proteasome (Ramirez et al., 2006; Park et al., 2011; Tan et al., 2011). The L1059R mutation that resides in transmembrane domain 9, predicted to disrupt this topology, also causes relocation to the endoplasmic reticulum and degradation by the proteasome (Park et al., 2011). The effects of the homozygous recessive missense mutation F182L and G504R in ATP13A2 have not been studied and are not intuitive (Di et al., 2007; Ning et al., 2008). Here we show in biochemical and cellular localization studies that the F182L and G504R mutations cause misfolding of ATP13A2 such that these proteins are retained in the endoplasmic reticulum and are degraded by the proteasome, likely by the ERAD-proteasome system. It is unclear why the F182L mutation would have such a significant effect on the structure of ATP13A2. It is a reasonably conservative mutation (hydrophobic residue to hydrophobic residue) that it is present in the first intermembrane loop with unknown function. On the other hand, the G504R is predicted to have a much more pronounced effect by introducing a positive charge in the second cytoplasmic loop before but in close proximity to the conversed DKTGTLT motif, where the D residue is involved in the high-energy aspartyl-phosphorl enzyme intermediate in the catalytic site (Scarborough, 1999; Kuhlbrandt, 2004). However, more detailed structural analysis of these regions is required to understand the consequences of these mutations. Nevertheless, their dramatic effects on protein stability and intracellular localization are consistent with the recessive mode of transmission.

ATP13A2 belongs to group 5 of the P-type ATPase protein family, which typically uses ATP hydrolysis to generate gradients of ions across membranes (Axelsen and Palmgren, 1998; Kuhlbrandt, 2004). The precise transport activity of ATP13A2 has not been directly assayed, although from the initial report of its protection against manganese toxicity in yeast (Gitler et al., 2009) it has been inferred that ATP13A2 may be a manganese transporter. Our

data from mammalian cells, in addition to other consistent data from yeast (Schmidt et al., 2009), indicate that ATP13A2 has a much broader function than simply acting to transport manganese. Not only can ATP13A2 protect against the toxicity of several specific divalent cations (Fig. 3; Schmidt et al., 2009), we also show that it has a dramatic general protective function against the toxicity associated with mitochondrial complex I impairment, oxidative stress, and proteasomal stress. The protective mechanism of ATP13A2 is unclear, but it is unlikely to be due solely to the direct activity as a divalent cation transporter, as previously suggested (Gitler et al., 2009). It would be difficult to envision how the sole activity of a lysosomal cation importer could have such a protective effect against the wide variety of cellular stresses assayed here. Alternatively, ATP13A2 may be involved in the import of a cofactor required for the function of lysosomal enzymes, thus increasing lysosomal activity and rendering cells more apt to deal with adverse conditions such as oxidative stress. In agreement with this notion, Usenovic et al. (2012) recently demonstrated that a loss or reduction in ATP13A2 expression results in impaired lysosomal degradation capacity. Because some P-type ATPase can transport substrates besides cations, such as phospholipids, we cannot exclude such a function for ATP13A2. We also cannot exclude the possibility that some of the effects of ATP13A2 are due to expression at lower levels in other organelles. Several recent studies suggest that ATP13A2 might have various direct or indirect effects on mitochondrial integrity (Vilarino-Guell et al., 2009; Ugolino et al., 2011; Grunewald et al., 2012). Altogether, these roles for ATP13A2 may explain the general protective effects seen here as well as in cultured neurons and yeast, in which ATP13A2 (or the *C. elegans* ortholog YPK9) expression suppresses α-synuclein toxicity (Gitler et al., 2009).

Overexpression of ATP13A2 did not inhibit some of the typical pathways that are involved in sensing cellular stress, and it did not inhibit pathways involved in apoptosis. In fact, for reasons that are unclear, the baseline activity of these pathways appears elevated in ATP13A2-overexpressing cells. It is possible that the expression of ATP13A2 alters some feedback mechanisms that regulate apoptosis and/or that ATP13A2 simply renders cells more resilient to cope with elevated basal activity of these pathways, but increasing numbers of studies demonstrate that partial activation of apoptotic pathways does not necessary lead to cell death. Nevertheless, the accumulation of markers for oxidized proteins was suppressed in ATP13A2-overexpressing cells. Therefore, it is possible that ATP13A2 enabled cells to survive the adverse stress better by reducing the levels of intracellular oxidative damage or enhancing the clearance of oxidatively damaged macromolecules. Consistent with this notion, a recessive single-nucleotide deletion mutation resulting in either exon skipping or a frameshift mutation in canine ATP13A2 was recently shown to be responsible for a form of adult-onset neuronal ceroid-lipofuscinosis in Tibetan terriers (Farias et al., 2011; Wohlke et al., 2011). Neuronal ceroid lipofucinoses are progressive neurodegenerative disease characterized by the accumulation of a variety of autofluorescent protein-aceous materials within lysosomes in the brain and other tissues. The disease in canines has some features strikingly similar to those in humans, such as generalized brain atrophy and cognitive decline (Farias et al., 2011; Wohlke et al., 2011); however, the affected animals do not develop parkinsonism or pyramidal dysfunction (Farias et al., 2011; Wohlke et al., 2011) but instead present with cerebellar ataxia. Although no brain autopsies

have been performed on patients with ATP13A2 mutations, a sural biopsy showed acute axonal degeneration and numerous cytoplasmic inclusion bodies resembling irregular lysosomes within Schwann cells (Paisan-Ruiz et al., 2010). Recently, an M810R mutation in ATP13A2 was identified in a kindred with the clinical and pathological (muscle and nerve biopsies) diagnosis of neuronal ceroid lipofuscinoses (Tome et al., 1985; Bras et al., 2012). Many human gene defects have been associated with neuronal ceroid lipofucinoses, and most are transmembrane proteins of unknown function or enzymes localized to lysosomes (Kousi et al., 2012). Therefore, it is tantalizing to hypothesize that the functions of ATP13A2 might be to import a cofactor required for the function of a lysosome enzyme(s).

The more general cellular protective effects of ATP13A2 shown here are consistent with the juvenile onset and the broader clinical presentation of patients with ATP13A2 pathological mutations, which include levodopa-induced parkinsonism, hallucinations, supranuclear vertical gaze, and dementia (Ramirez et al., 2006; Di et al., 2007; Ning et al., 2008; Santoro et al., 2011). The finding that ATP13A2 may be elevated in surviving dopaminergic neurons in PD also suggests a protective role for this protein (Ramirez et al., 2006; Ramonet et al., 2012), but this finding is controversial (Vilarino-Guell et al., 2009). Nevertheless, ATP13A2's protection against α-synuclein toxicity (Gitler et al., 2009) and many other stresses associated with PD lends credence to the notion that ATP13A2 plays an important protective role in PD, but further studies are needed to understand the mechanism better.

Acknowledgments

Contract grant sponsor: National Institute of Neurological Disorders and Stroke; Contract grant number: NS053488.

References

Axelsen KB, Palmgren MG. Evolution of substrate specificities in the P-type ATPase superfamily. J Mol Evol. 1998; 46:84–101. [PubMed: 9419228]

Braak H, Bohl JR, Muller CM, Rub U, de Vos RA, Del TK. Stanley Fahn Lecture 2005: the staging procedure for the inclusion body pathology associated with sporadic Parkinson's disease reconsidered. Mov Disord. 2006; 21:2042–2051. [PubMed: 17078043]

Bras J, Verloes A, Schneider SA, Mole SE, Guerreiro RJ. Mutation of the parkinsonism gene ATP13A2 causes neuronal ceroid-lipofuscinosis. Hum Mol Genet. 2012; 21:2646–2650. [PubMed: 22388936]

Chaudhuri KR, Healy DG, Schapira AH. Non-motor symptoms of Parkinson's disease: diagnosis and management. Lancet Neurol. 2006; 5:235–245. [PubMed: 16488379]

Cromford ME, Chang L, Miller BL. The neuropathology of Parkinsonism: an overview. Brain Cogn. 1995; 28:321–341. [PubMed: 8546858]

Crosiers D, Ceulemans B, Meeus B, Nuytemans K, Pals P, Van BC, Cras P, Theuns J. Juvenile dystonia-parkinsonism and dementia caused by a novel ATP13A2 frameshift mutation. Parkinsonism Rel Disord. 2011; 17:135–138.

Dawson TM, Dawson VL. Molecular pathways of neurodegeneration in Parkinson's disease. Science. 2003; 302:819–822. [PubMed: 14593166]

Di FA, Chien HF, Socal M, Giraudo S, Tassorelli C, Iliceto G, Fabbrini G, Marconi R, Fincati E, Abbruzzese G, Marini P, Squitieri F, Horstink MW, Montagna P, Libera AD, Stocchi F, Goldwurm S, Ferreira JJ, Meco G, Martignoni E, Lopiano L, Jardim LB, Oostra BA, Barbosa ER, Bonifati V. ATP13A2 missense mutations in juvenile parkinsonism and young onset Parkinson disease. Neurology. 2007; 68:1557–1562. [PubMed: 17485642]

Dick FD, De PG, Ahmadi A, Scott NW, Prescott GJ, Bennett J, Semple S, Dick S, Counsell C, Mozzoni P, Haites N, Wettinger SB, Mutti A, Otelea M, Seaton A, Soderkvist P, Felice A. Environmental risk factors for Parkinson's disease and parkinsonism: the geoparkinson study. Occup Environ Med. 2007; 64:666–672. [PubMed: 17332139]

Eiberg H, Hansen L, Korbo L, Nielsen I, Svenstrup K, Bech S, Pinborg L, Friberg L, Hjermind L, Olsen O, Nielsen J. Novel mutation in ATP13A2 widens the spectrum of Kufor-Rakeb syndrome (PARK9). Clin Genet. 2011 (E-pub ahead of print).

Elbaz A, Clavel J, Rathouz PJ, Moisan F, Galanaud JP, Delemotte B, Alperovitch A, Tzourio C. Professional exposure to pesticides and Parkinson disease. Ann Neurol. 2009; 66:494–504. [PubMed: 19847896]

Farias FH, Zeng R, Johnson GS, Wininger FA, Taylor JF, Schnabel RD, McKay SD, Sanders DN, Lohi H, Seppala EH, Wade CM, Lindblad-Toh K, O'Brien DP, Katz ML. A truncating mutation in ATP13A2 is responsible for adult-onset neuronal ceroid lipofuscinosis in Tibetan terriers. Neurobiol Dis. 2011; 42:468–474. [PubMed: 21362476]

Forman MS, Lee VM, Trojanowski JQ. Nosology of Parkinson's disease: looking for the way out of a quackmire. Neuron. 2005; 47:479–482. [PubMed: 16102530]

Forno LS. Neuropathology of Parkinson's disease. J Neuropathol Exp Neurol. 1996; 55:259–272. [PubMed: 8786384]

Gelb DJ, Oliver E, Gilman S. Diagnostic criteria for Parkinson disease. Arch Neurol. 1999; 56:33–39. [PubMed: 9923759]

Giasson BI, Lee VMY. Are ubiquitination pathways central to Parkinson's disease? Cell. 2003; 114:1–8. [PubMed: 12859888]

Giasson BI, Ischiropoulos H, Lee VMY, Trojanoswki JQ. The relationship between oxidative/nitrative stress and pathological inclusions in Alzheimer's and Parkinson's diseases. Free Radic Biol Med. 2002; 32:1264–1275. [PubMed: 12057764]

Gitler AD, Chesi A, Geddie ML, Strathearn KE, Hamamichi S, Hill KJ, Caldwell KA, Caldwell GA, Cooper AA, Rochet JC, Lindquist S. Alpha-synuclein is part of a diverse and highly conserved interaction network that includes PARK9 and manganese toxicity. Nat Genet. 2009; 41:308–315. [PubMed: 19182805]

Grunewald A, Arns B, Seibler P, Rakovic A, Munchau A, Ramirez A, Sue CM, Klein C. ATP13A2 mutations impair mitochondrial function in fibroblasts from patients with Kufor-Rakeb syndrome. Neurobiol Aging. 2012; 33:1843.e1–7. [PubMed: 22296644]

Hampshire DJ, Roberts E, Crow Y, Bond J, Mubaidin A, Wriekat AL, Al-Din A, Woods CG. Kufor-Rakeb syndrome, pallido-pyramidal degeneration with supranuclear upgaze paresis and dementia, maps to 1p36. J Med Genet. 2001; 38:680–682. [PubMed: 11584046]

Henchcliffe C, Beal MF. Mitochondrial biology and oxidative stress in Parkinson disease pathogenesis. Nat Clin Pract Neurol. 2008; 4:600–609. [PubMed: 18978800]

Kousi M, Lehesjoki AE, Mole SE. Update of the mutation spectrum and clinical correlations of over 360 mutations in eight genes that underlie the neuronal ceroid lipofuscinoses. Hum Mutat. 2012; 33:42–63. [PubMed: 21990111]

Kuhlbrandt W. Biology, structure and mechanism of P-type ATPases. Nat Rev Mol Cell Biol. 2004; 5:282–295. [PubMed: 15071553]

Lai BC, Marion SA, Teschke K, Tsui JK. Occupational and environmental risk factors for Parkinson's disease. Parkinsonism Rel Disord. 2002; 8:297–309.

Lesage S, Brice A. Parkinson's disease: from monogenic forms to genetic susceptibility factors. Hum Mol Genet. 2009; 18:R48–R59. [PubMed: 19297401]

Martin I, Dawson VL, Dawson TM. Recent advances in the genetics of Parkinson's disease. Annu Rev Genomics Hum Genet. 2011; 12:301–325. [PubMed: 21639795]

Ning YP, Kanai K, Tomiyama H, Li Y, Funayama M, Yoshino H, Sato S, Asahina M, Kuwabara S, Takeda A, Hattori T, Mizuno Y, Hattori N. PARK9-linked parkinsonism in eastern Asia: mutation detection in ATP13A2 and clinical phenotype. Neurology. 2008; 70:1491–1493. [PubMed: 18413573]

Paisan-Ruiz C, Guevara R, Federoff M, Hanagasi H, Sina F, Elahi E, Schneider SA, Schwingenschuh P, Bajaj N, Emre M, Singleton AB, Hardy J, Bhatia KP, Brandner S, Lees AJ, Houlden H. Early-

onset L-dopa-responsive parkinsonism with pyramidal signs due to ATP13A2, PLA2G6, FBXO7 and spatacsin mutations. Mov Disord. 2010; 25:1791–1800. [PubMed: 20669327]

Park JS, Mehta P, Cooper AA, Veivers D, Heimbach A, Stiller B, Kubisch C, Fung VS, Krainc D, Mackay-Sim A, Sue CM. Pathogenic effects of novel mutations in the P-type ATPase ATP13A2 (PARK9) causing Kufor-Rakeb syndrome, a form of early-onset parkinsonism. Hum Mutat. 2011; 32:956–964. [PubMed: 21542062]

Poewe W. Non-motor symptoms in Parkinson's disease. Eur J Neurol. 2008; 15(Suppl 1):14–20. [PubMed: 18353132]

Ramirez A, Heimbach A, Grundemann J, Stiller B, Hampshire D, Cid LP, Goebel I, Mubaidin AF, Wriekat AL, Roeper J, Al-Din A, Hillmer AM, Karsak M, Liss B, Woods CG, Behrens MI, Kubisch C. Hereditary parkinsonism with dementia is caused by mutations in ATP13A2, encoding a lysosomal type 5 P-type ATPase. Nat Genet. 2006; 38:1184–1191. [PubMed: 16964263]

Ramonet D, Podhajska A, Stafa K, Sonnay S, Trancikova A, Tsika E, Pletnikova O, Troncoso JC, Glauser L, Moore DJ. PARK9-associated ATP13A2 localizes to intracellular acidic vesicles and regulates cation homeostasis and neuronal integrity. Hum Mol Genet. 2012; 21:1725–1743. [PubMed: 22186024]

Ramsey CP, Giasson BI. Role of mitochondrial dysfunction in Parkinson's disease: Implications for treatment. Drugs Aging. 2007; 24:95–105. [PubMed: 17313198]

Santoro L, Breedveld GJ, Manganelli F, Iodice R, Pisciotta C, Nolano M, Punzo F, Quarantelli M, Pappata S, Di FA, Oostra BA, Bonifati V. Novel ATP13A2 (PARK9) homozygous mutation in a family with marked phenotype variability. Neurogenetics. 2011; 12:33–39. [PubMed: 20853184]

Scarborough GA. Structure and function of the P-type ATPases. Curr Opin Cell Biol. 1999; 11:517–522. [PubMed: 10449329]

Schmidt K, Wolfe DM, Stiller B, Pearce DA. Cd^{2+}, Mn^{2+}, Ni^{2+} and Se^{2+} toxicity to Saccharomyces cerevisiae lacking YPK9p the orthologue of human ATP13A2. Biochem Biophys Res Commun. 2009; 383:198–202. [PubMed: 19345671]

Schultheis PJ, Hagen TT, O'Toole KK, Tachibana A, Burke CR, McGill DL, Okunade GW, Shull GE. Characterization of the P5 subfamily of P-type transport ATPases in mice. Biochem Biophys Res Commun. 2004; 323:731–738. [PubMed: 15381061]

Simuni, T.; Hurtig, HI. Parkinson's disease: the clinical picture. In: Clark, CM.; Trojanoswki, JQ., editors. Neurodegenerative dementias. New York: McGraw-Hill; 2000. p. 193-203.

Tan J, Zhang T, Jiang L, Chi J, Hu D, Pan Q, Wang D, Zhang Z. Regulation of intracellular manganese homeostasis by Kufor-Rakeb syndrome-associated ATP13A2 protein. J Biol Chem. 2011; 286:29654–29662. [PubMed: 21724849]

Tome FM, Brunet P, Fardeau M, Hentati F, Reix J. Familial disorder of the central and peripheral nervous systems with particular cytoplasmic lamellated inclusions in peripheral nerves, muscle satellite cells, and blood capillaries. Acta Neuropathol. 1985; 68:209–217. [PubMed: 4082923]

Ugolino J, Fang S, Kubisch C, Monteiro MJ. Mutant Atp13a2 proteins involved in parkinsonism are degraded by ER-associated degradation and sensitize cells to ER-stress induced cell death. Hum Mol Genet. 2011; 20:3565–3577. [PubMed: 21665991]

Usenovic M, Tresse E, Mazzulli JR, Taylor JP, Krainc D. Deficiency of ATP13A2 leads to lysosomal dysfunction, alpha-synuclein accumulation, and neurotoxicity. J Neurosci. 2012; 32:4240–4246. [PubMed: 22442086]

Vilarino-Guell C, Soto AI, Lincoln SJ, Ben YS, Kefi M, Heckman MG, Hulihan MM, Chai H, Diehl NN, Amouri R, Rajput A, Mash DC, Dickson DW, Middleton LT, Gibson RA, Hentati F, Farrer MJ. ATP13A2 variability in Parkinson disease. Hum Mutat. 2009; 30:406–410. [PubMed: 19085912]

Weingarten LS, Dave H, Li H, Crawford DA. Developmental expression of P5 ATPase mRNA in the mouse. Cell Mol Biol Lett. 2012; 17:153–170. [PubMed: 22207337]

Westerlund M, Hoffer B, Olson L. Parkinson's disease: exit toxins, enter genetics. Prog Neurobiol. 2010; 90:146–156. [PubMed: 19925845]

Williams DR, Hadeed A, al-Din AS, Wreikat AL, Lees AJ. Kufor Rakeb disease: autosomal recessive, levodopa-responsive parkinsonism with pyramidal degeneration, supranuclear gaze palsy, and dementia. Mov Disord. 2005; 20:1264–1271. [PubMed: 15986421]

Wohlke A, Philipp U, Bock P, Beineke A, Lichtner P, Meitinger T, Distl O. A one base pair deletion in the canine ATP13A2 gene causes exon skipping and late-onset neuronal ceroid lipofuscinosis in the Tibetan terrier. PLoS Genet. 2011; 7:e1002304. [PubMed: 22022275]

Zhang Y, Dawson VL, Dawson TM. Oxidative stress and genetics in the pathogenesis of Parkinson's disease. Neurobiol Dis. 2000; 7:240–250. [PubMed: 10964596]

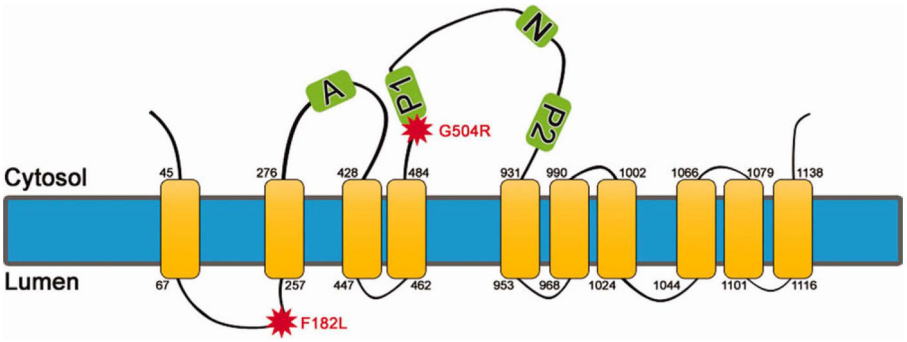

Fig. 1.

Schematic representation of ATP13A2. ATP13A2 (PARK9) is predicted to be a 10-transmembrane protein, as shown. In some models, one or two additional transmembrane domains have been proposed (Schultheis et al., 2004). The actuator domain is shown as A. The phosphorylation domains involved in the high-energy aspartyl-phosphorl enzyme intermediate in the catalytic site are shown as P1 and P2. The nucleotide domain is shown as N. The locations of the F182L and G504R mutations are indicated by stars. [Color figure can be viewed in the online issue, which is available at wileyonlinelibrary.com.]

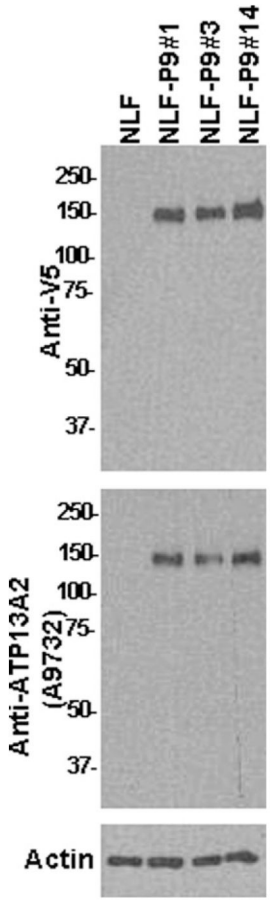

Fig. 2.

Western blot analysis demonstrating the expression of ATP13A2 in stable NLF cells clones. Western blot analysis with anti-V5 antibody or anti-ATP13A2 antibody A9732 showing the expression of WT ATP13A2 in three stable NLF cell lines (clones NLF-P9 No. 1, NLF-P9 No. 3, and NLF-P9 No. 14). One lane was loaded with protein extract from nontransfected cells. Ten micrograms of total cell extract lysed in 3% SDS was loaded in each lane of 8% polyacrylamide gels. Membranes were probed with either anti-V5 antibody or anti-ATP13A2 antibody A9732. The mobility of molecular mass markers is indicated at left. An immunoblot with an antiactin antibody is shown as a loading control.

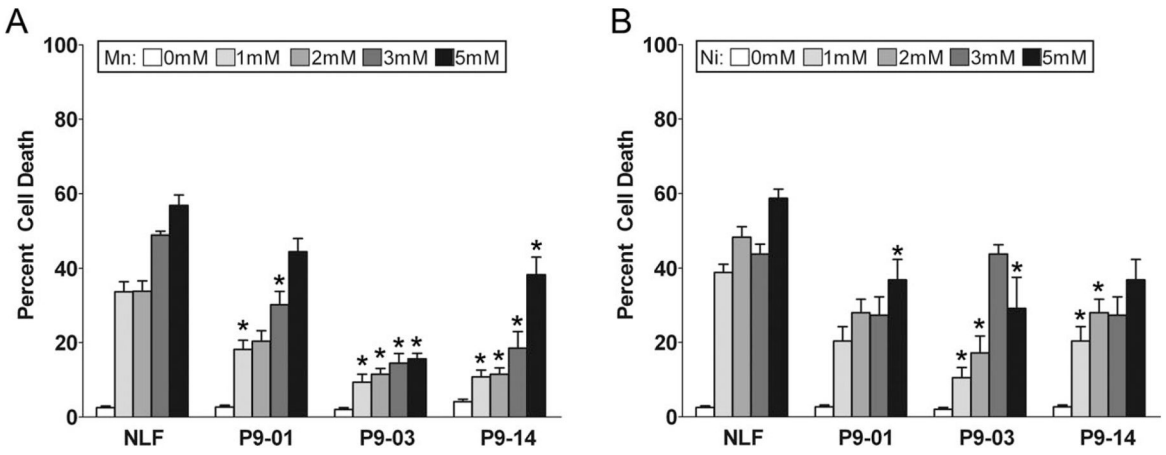

Fig. 3.

Expression of ATP13A2 protects against Mn and Ni toxicity. NLF cells stably expressing WT ATP13A2 (clones NLF-P9 No. 1, NLF-P9 No. 3, and NLF-P9 No. 14) and native NLF cells were treated for 24 hr with various concentration of $MnCl_2$ (**A**) or $NiCl_2$ (**B**). Trypan blue exclusion assays were performed to assess viability, and results are plotted as the percentage of dead cells. Error bars represent SEM (n = 6). ★$P = 0.01$.

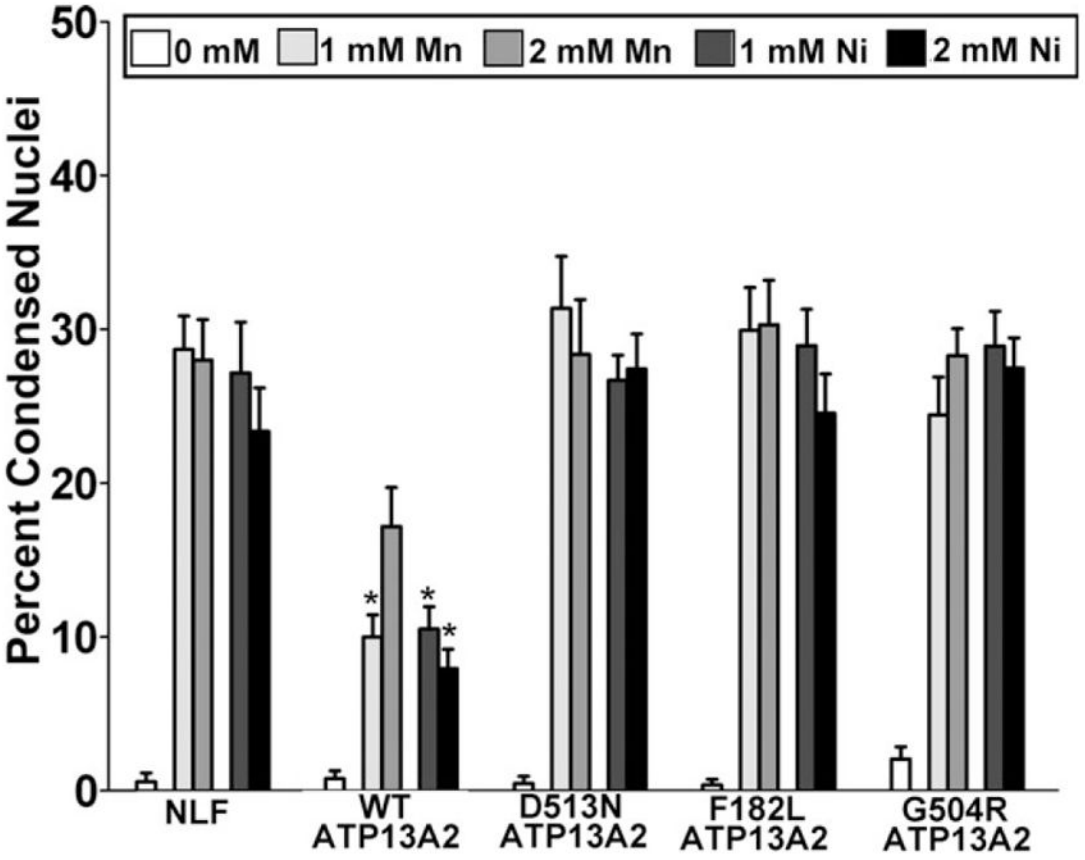

Fig. 4.

F182L and G504R ATP13A2 do not protect against Mn and Ni toxicity. NLF cells were transiently transfected to express WT ATP13A2, disease-associated mutants F182L or G504R ATP13A2, and an "enzyme-dead" D513N mutant. Transfected cells were challenged for 24 hr with 1 or 2 mM $MnCl_2$ or $NiCl_2$ as indicated, and the percentage of transfected cells with condensed/apoptotic nuclei was assessed by cotransfection with an eGFP-expressing plasmid and DAPI staining. As a baseline control, NLF cells were cotransfected with an empty expression vector and eGFP. Error bars represent SEM (n = 3). ★$P = 0.01$.

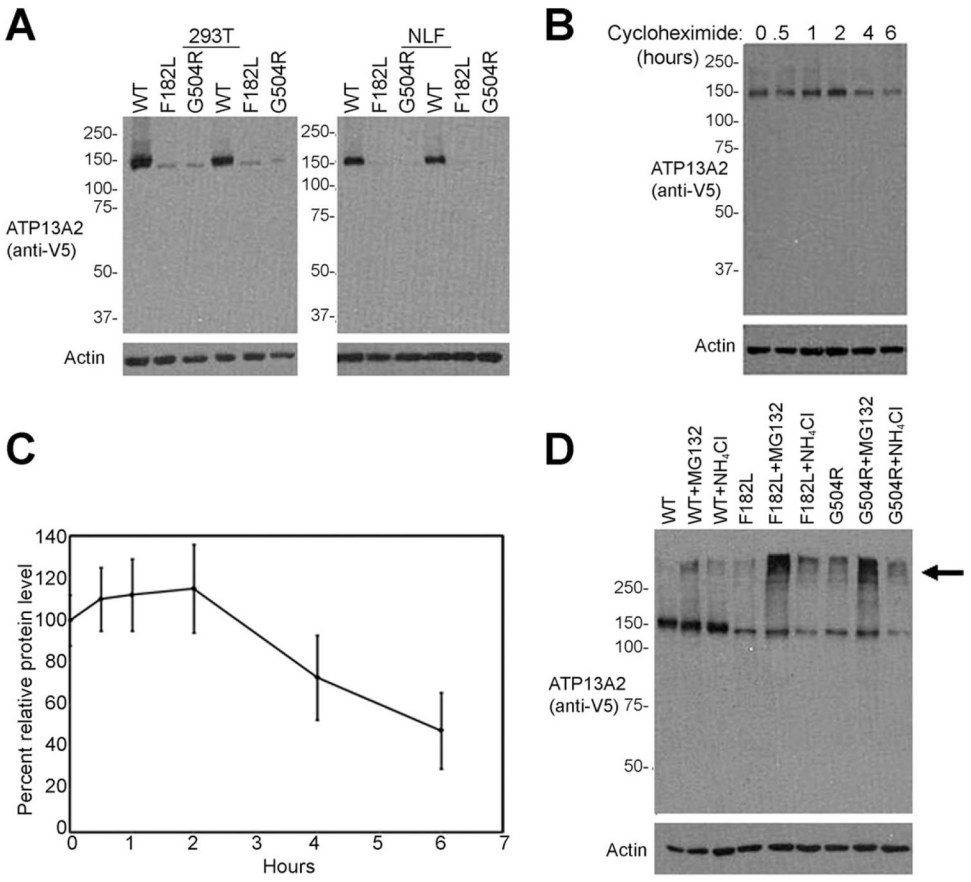

Fig. 5.

F182L and G504R ATP132A are unstable are and degraded by the proteasome. **A**: 293T cells or NLF cells, as indicate above each blot, were transfected with WT, F182L, or G504R ATP13A2 expression plasmids, and the steady-state expression of these proteins was assessed by Western blotting analysis. Data shown represent experiments performed in duplicate for each cell line. Blots were also probed with an antiactin as a loading control. **B,C**: With 293T cells, the relative turnover of WT ATP13A2 was assessed by using the translation inhibitor cycloheximide for the times indicated. A representative analysis is shown in B, and quantitative analysis is presented in C. **D**: 293T cells were transfected with WT, F182L, or G504R ATP13A2 expression plasmids and cultured for 30 hr. Cells were left untreated or were treated with 25 μM MG132 or 25 mM NH_4Cl for 6 hr before harvesting in 3% SDS, followed by Western blot analysis. Ten micrograms of total protein extracts was loaded on each lane of 8% polyacrylamide gels. The accumulation of ATP13A2 aggregates at the top of the resolving gel is indicated by an arrow.

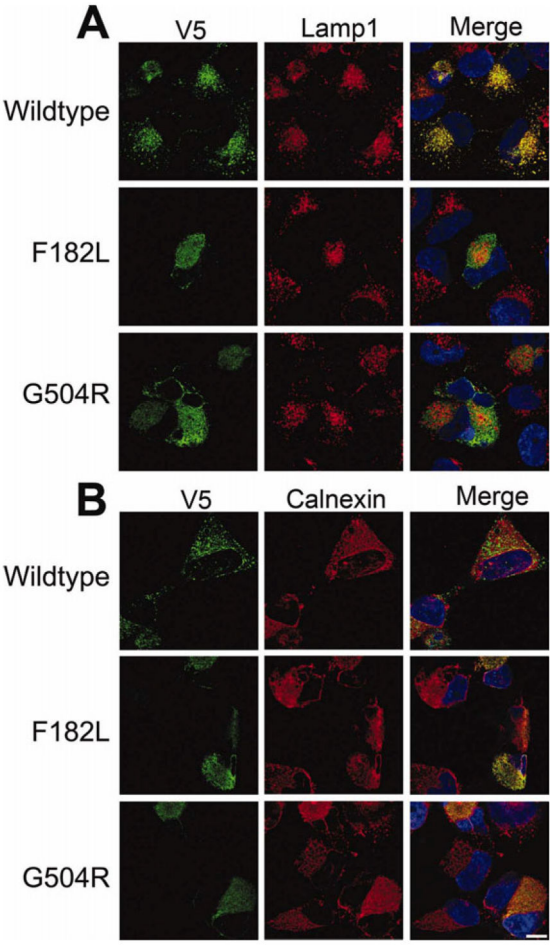

Fig. 6.

Confocal microscopic analysis of the localization of WT and mutant ATP13A2. NLF cells were transfected with expression plasmids for V5-tagged WT, F182L, or G504R ATP13A2. Double immunofluorescence was performed between anti-V5 antibodies (green) and Lamp1 (red; **A**) or calnexin (red; **B**). Overlays are shown on the right columns with cells counterstained with Hoechst 33342 (blue). Scale bar = 10 μm. [Color figure can be viewed in the online issue, which is available at wileyonlinelibrary.com.]

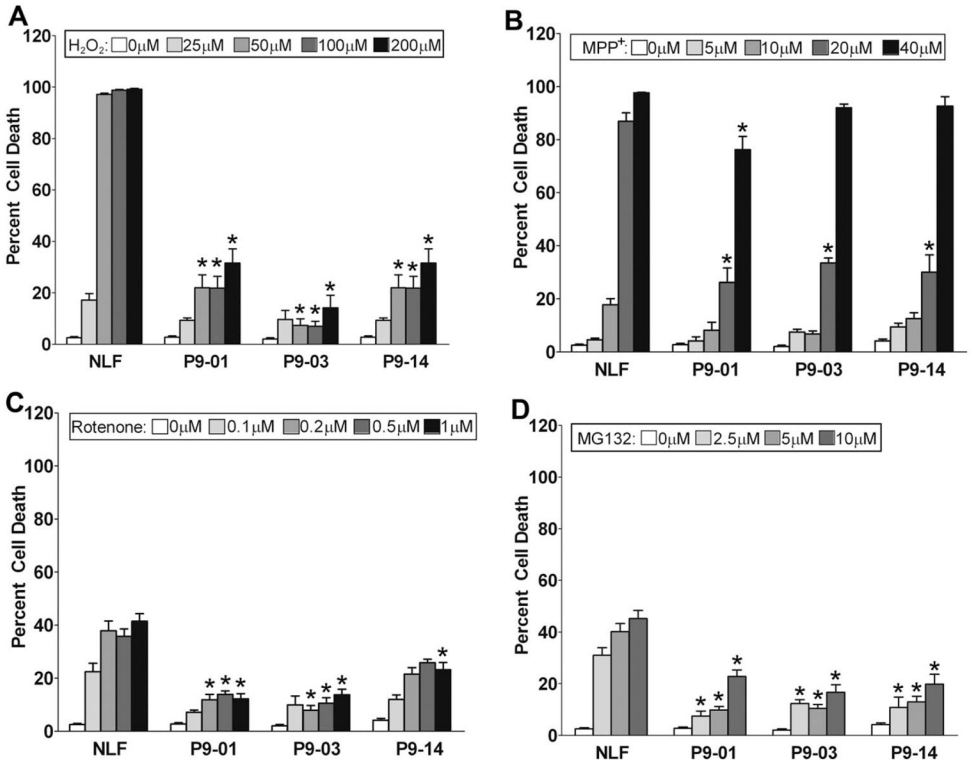

Fig. 7.

Expression of ATP13A2 protects against various cellular insults. NLF stable clones expressing WT ATP13A2 (clones NLF-P9 No. 1, NLF-P9 No. 3, and NLF-P9 No. 14) and native NLF cells were treated for 24 hr with various concentrations of H_2O_2 (**A**), MPP^+ (**B**), rotenone (**C**), or MG132 (**D**). Trypan blue exclusion assays were performed to assess viability. Results are plotted as the percentage of dead cells. Error bars represent SEM (n = 6). ★$P = 0.01$.

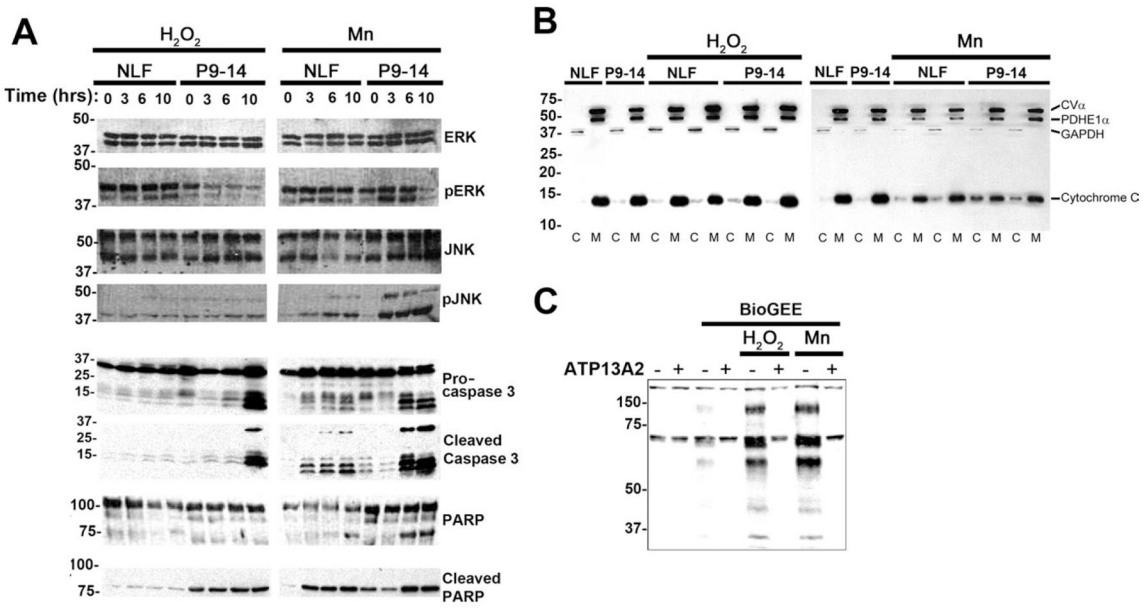

Fig. 8.

Analysis of the effects of ATP13A2 expression on signal transduction pathways under conditions of cellular stress. **A**: Native NLF cells and NLF P9–14 cells were challenged with 50 μM H_2O_2 or 1 mM MnCl2 for 0, 3, 6, or 10 hr. Western blot analysis of various components of signal transduction pathways were performed with the antibodies indicated. Equal protein amounts were loaded in each lane of SDS-polyacrylamide gels. **B**: Biochemical assay for the release of cytochrome C in the cytosol. Cells were treated with 50 μM H_2O_2 or 1 mM $MnCl_2$ for 6 hr. C, cytosolic fraction; M, mitochondrial fraction; CVα, complex Vα; PDHE1α, pyruvate dehydrogenase E1α; GAPHD, glyceraldehyde 3-phosphate dehydrogenase. **C**: Native NLF cells (−) and cells overexpressing ATP13A2 (NLF P9–14; +) were assayed for intracellular oxidative damage by glutathione incorporation with the BioGEE assay. Cells were untreated or treated with 50 μM H_2O_2 or 1 mM $MnCl_2$ for 6 hr.